Supplement of Atmos. Chem. Phys., 17, 3699–3712, 2017
http://www.atmos-chem-phys.net/17/3699/2017/
doi:10.5194/acp-17-3699-2017-supplement

Supplement of

Wintertime enhancements of sea salt aerosol in polar regions consistent with a sea ice source from blowing snow

Jiayue Huang and Lyatt Jaeglé

Correspondence to: Lyatt Jaeglé (jaegle@uw.edu)

1 Open ocean emissions over cold polar waters during summer

Figure S1 compares observed SSA mass concentrations at Barrow, Zeppelin, Neumayer, and Dumont d'Urville to the GEOS-Chem simulation (ORIG simulation) with open ocean SSA emissions only. During warm months when local sea ice extent is at a minimum and open ocean emissions dominate SSA mass concentrations, the model overestimates observations by a factor of 2. We hypothesize that this overestimate indicates a stronger suppression of SSA emissions over cold polar waters than accounted for in the SST dependence of Jaeglé et al. (2011) in which most of the observations used were for SST>5°C (see Fig. 6 in Jaeglé et al., 2011). A simulation in which we assume f(SST)=0.25 for SST<5^{o}C results in improved agreement with observed summertime SSA mass concentrations and does not affect SSA mass concentrations during winter. This is the standard simulation (STD) used in the main text.

2 Influence of assumed number of particles produced per snowflake on the size distributions of SSA from blowing snow

Figure S2 shows the seasonal variations of observed submicron and supermicron SSA mass concentrations at Barrow, Alaska. The observed submicron SSA concentrations at Barrow maximize in winter, while the supermicron SSA concentrations have their maximum during summer (Quinn et al. 2002). We examine how the size distribution of SSA from blowing snow is affected by assumptions on the number of particles produced per snowflake (N). For N=1, the blowing snow simulation predicts submicron SSA concentrations <0.3 μg m^{-3}, a factor of 2-3 lower than observed concentrations of 0.5-1.3 μg m^{-3} for November-March. Increasing N to a value of 5 shifts more of the blowing snow SSA mass to submicron aerosol and leads to better agreement with observed submicron SSA concentration at Barrow, without much change in the supermicron SSA. The blowing snow simulation with N=5 corresponds to the STD-SNOW simulation in the main text.

3 Sensitivity simulations on wind thresholds for frost flower formation

We perform a sensitivity simulation for frost flower formation, in which we impose a wind threshold of 5 m/s beyond which frost flower formation and emission are inhibited in the model: STD-FF (<5 m/s). This simulation assumes that strong winds inhibit frost flower formation and bury existing frost flowers with snow (Perovich and Richeter-Menge, 1994; Rankin et al., 2000). The frost flower emission in this sensitivity simulation has a scaling factor 5 times larger than the one used in STD-FF (=1×10^{6} m^{2} s^{-1}, Xu et al. 2013), in order to reproduce the SSA mass concentrations observed at Alert. The resulting simulation is shown in Fig. S3. With this wind threshold, the new frost flower simulation underestimates the SSA mass concentration by factors of 2-3 at Barrow in December-January, and overestimates the SSA mass concentrations by a factor of 2 at Alert in December-March. At the other sites, the influence of frost flower remains very small, and thus cannot fully explain the wintertime SSA enhancements. Therefore, imposing a wind threshold for frost flower emission does not lead to a better model agreement and does not alter our conclusions on frost flower simulations.

4 Daily variability of SSA mass concentration observed at Alert and Dumont d'Urville

Figure S4 compares observed and modeled variations in SSA mass concentrations at Alert and Dumont d'Urville for the year 2001. Observations are weekly at Alert and daily at Dumont d'Urville. At Alert (Fig. S4a) observed concentrations of SSA vary between 0.3 and 2 µg m^{-3} between November and early June, while during the rest of the year observed concentrations remain below 0.1 µg m^{-3}. The blowing snow simulation (STD-SNOW) captures the timing of some of the large episodic enhancements in SSA: in mid-January, early and late April, June, and November. This variability is not well reproduced by the frost flower simulation. At Dumont d'Urville (Fig. S4b), the influence of frost flowers is minor, but the blowing snow simulation reproduces to some extent the variability and magnitude of observed SSA mass concentrations. Fig. S3c shows that the SO_4^{2-}/Na^+ ratio at Dumont d'Urville has winter minima (<0.25), and is particularly low when elevated levels of SSA mass concentrations were observed during winter. This is consistent with the low/negative non-sea-salt SO_4^{2-} levels found in aerosol samples over polar regions in several previous studies (Jourdain et al., 2001; Rankin et al., 2000; Wagenbach et al., 1998), which is related to the sulphate depletion in snow and frost flower on sea ice (Krnavek et al., 2012; Rankin et al., 2000; Seguin et al., 2014).

5 Sensitivity simulation including both blowing snow and frost flower emissions

Figure S5 compares observed SSA mass concentrations at Barrow, Alert, Zeppelin, Neumayer, and Dumont d'Urville to a simulation including open ocean, blowing snow, and frost flowers (STD-SNOW-FF). Overall, the combined influence of blowing snow and frost flowers in the model does not yield a better model agreement with the observations (with NMB, normalized mean bias, ranging from 12% to 81%) compared to blowing snow simulation (STD-SNOW in the main text, with NMB ranging from -2% to +25%). In particular, combining the influence of blowing snow and frost flowers in the model leads to factor of 2-3 overestimates of the SSA mass concentrations at Barrow in Jan-Mar and at Alert in Dec-Mar. At the other three polar sites, the influence of frost flowers is very small and thus the STD-SNOW-FF simulation is similar to the blowing snow simulation (STD-SNOW).

6 Global SSA budgets for the open ocean, blowing snow and frost flower simulation

Table S1 summarizes the global annual budget for SSA for the three sources considered in this study for the year 2005.

Table S1. Global budgets of SSA generated by the open ocean, blowing snow, and frost flowers for the year 2005.

	Open Ocean (STD)			Blowing Snow			Frost Flowers
	0.01-0.5 µm	0.5-4 µm	Total	0.01-0.5 µm	0.5-4 µm	Total	0.01-0.5 µm
Emission (Tg/yr)	52	1957	2009	3.8	3.6	7.4	0.49
Dry deposition (Tg/yr)	4.0	804	808	0.93	1.6	2.5	0.21
Wet deposition (Tg/yr)	49	1262	1311	3.0	2.2	5.2	0.32
Lifetime (days)	2.1	0.44	0.48	4.2	0.6	2.4	5.1
Burden (Gg)	297	2477	2774	45	6.0	51	7.4
Surface concentration (µg m^{-3})	0.6	5.7	6.3	0.078	0.020	0.098	0.02

References

Jaeglé, L., Quinn, P. K., Bates, T. S., Alexander, B., and Lin, J.-T.: Global distribution of sea salt aerosols: new constraints from in situ and remote sensing observations, Atmos. Chem. Phys., 11, 3137-3157, doi:10.5194/acp-11-3137-2011, 2011.

Jourdain, B. and Legrand, M.: Seasonal variations of atmospheric dimethylsulfide, dimethylsulfoxide, sulfur dioxide, methanesul- fonate, and non-sea-salt sulfate aerosols at Dumont d'Urville (coastal Antartctica) (December 1998 to July 1999), J. Geophys. Res., 106, 14391–14408, 2001.

Krnavek, L., Simpson, W. R., Carlson, D., Domine ́, F., Douglas, T. A., and Sturm, M.: The chemical composition of surface snow in the Arctic: examining marine, terrestrial, and atmospheric influence, Atmos. Environ., 50, 349–359, doi:10.1016/j.atmosenv.2011.11.033, 2012.

Perovich, D. K. and Richter-Menge, J. A.: Surface characteristics of lead ice, J. Geophys. Res., 99, 16341–16350, doi:10.1029/94JC01194, 1994.

Quinn, P. K., Miller, T. L., Bates, T. S., Ogren, J. A., Andrews, E., and Shaw, G. E.: A three-year record of simultaneously measured aerosol chemical and optical properties at Barrow, Alaska, J. Geophys. Res., 107, doi:10.1029/2001JD001248, 2002.

Rankin, A. M., Auld, V., and Wolff, E. W.: Frost flowers as a source of fractionated sea salt aerosol in the polar regions, Geophys. Res. Lett., 27, 3469–3472, doi:10.1029/2000GL011771, 2000.

Seguin, A.M., Norman, A.L. and Barrie, L.: Evidence of sea ice source in aerosol sulfate loading and size distribution in the Canadian High Arctic from isotopic analysis, J. Geophys. Res. Atmos., 119, 1087–1096, doi:10.1002/2013JD020461, 2014.

Wagenbach, D., Ducroz, F., Mulvaney, R., Keck, L., Minikin, A., Legrand, M., Hall, J. S., and Wolff, E. W.: Sea-salt aerosol in coastal Antarctic regions, J. Geophys. Res., 103, 10 961–10 974, 1998.

Xu, L., Russell, L. M., Somerville, R. C. J., and Quinn, P. K.: Frost flower aerosol effects on Arctic wintertime longwave cloud radiative forcing, J. Geophys. Res.-Atmos., 118, 13282–13291, doi:10.1002/2013JD020554, 2013.

Yang, X., Pyle, J. A., and Cox, R. A.: Sea salt aerosol production and bromine release: Role of snow on sea ice, Geophys. Res. Lett., 35, L16815, doi:10.1029/2008GL034536, 2008.

Yang, X., Pyle, J. A., Cox, R. A., Theys, N., and Van Roozendael, M.: Snow-sourced bromine and its implications for polar tropospheric ozone, Atmos. Chem. Phys., 10, 7763–7773, doi:10.5194/acp-10-7763-2010, 2010.

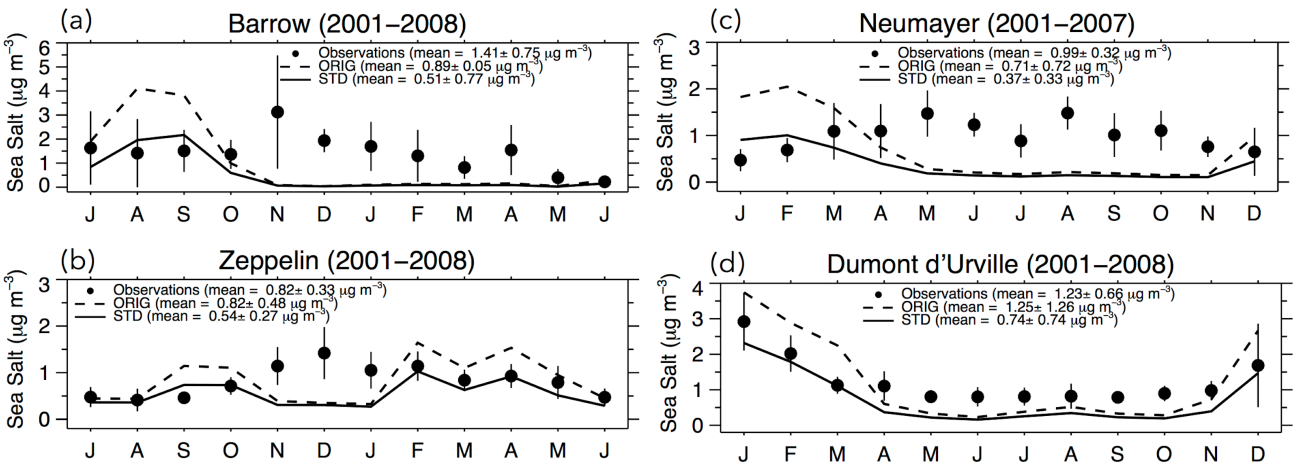

Figure S1: Monthly mean surface SSA mass concentrations at (a) Barrow, (b) Zeppelin, (c) Neumayer and (d) Dumont d'Urville. The observed mean concentrations are indicated with filled black circles, while the lines are for the GEOS-Chem model. The original GEOS-Chem simulation (ORIG) is shown with a black dashed line, while the standard simulation (STD) with enhanced SSA suppression for SST< 5°C is shown by the black line.

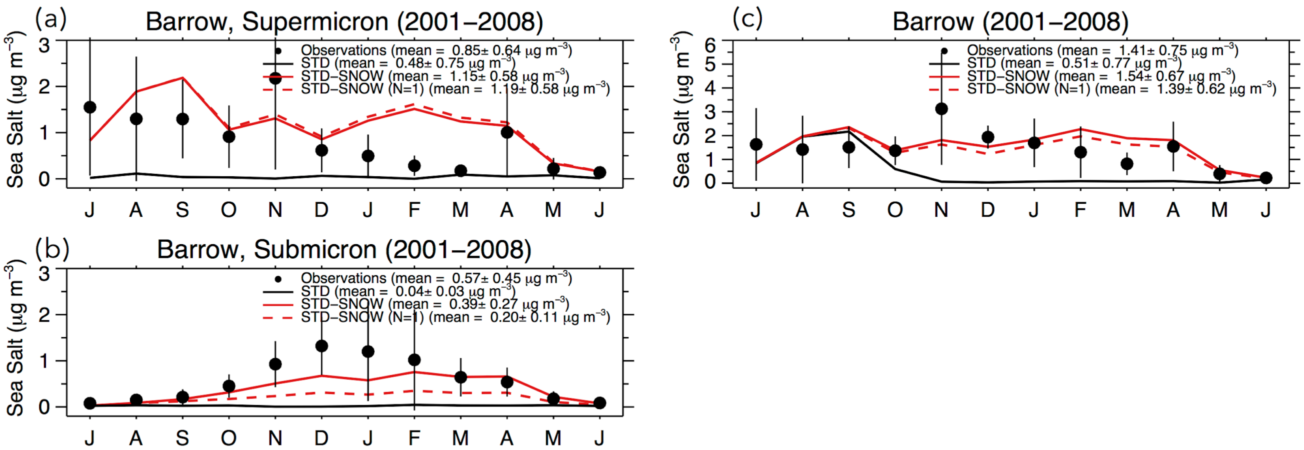

Figure S2: Monthly mean super-micron (a), sub-micron (b) and total (c) surface mass concentrations of SSA at Barrow (2001-2008). Note that the seasonal cycles are centered over local winter. The observed mean concentrations are indicated with black circles, while lines are for the concentrations in GEOS-Chem (STD: black line; STD-SNOW: red line; STD-SNOW (N=1): red dashed line). The STD-SNOW simulations assumes that the number of SSA particles per snowflake is N=5, while the STD-SNOW (N=1) assumes N=1. The black vertical lines correspond to the standard deviations of monthly means for observations.

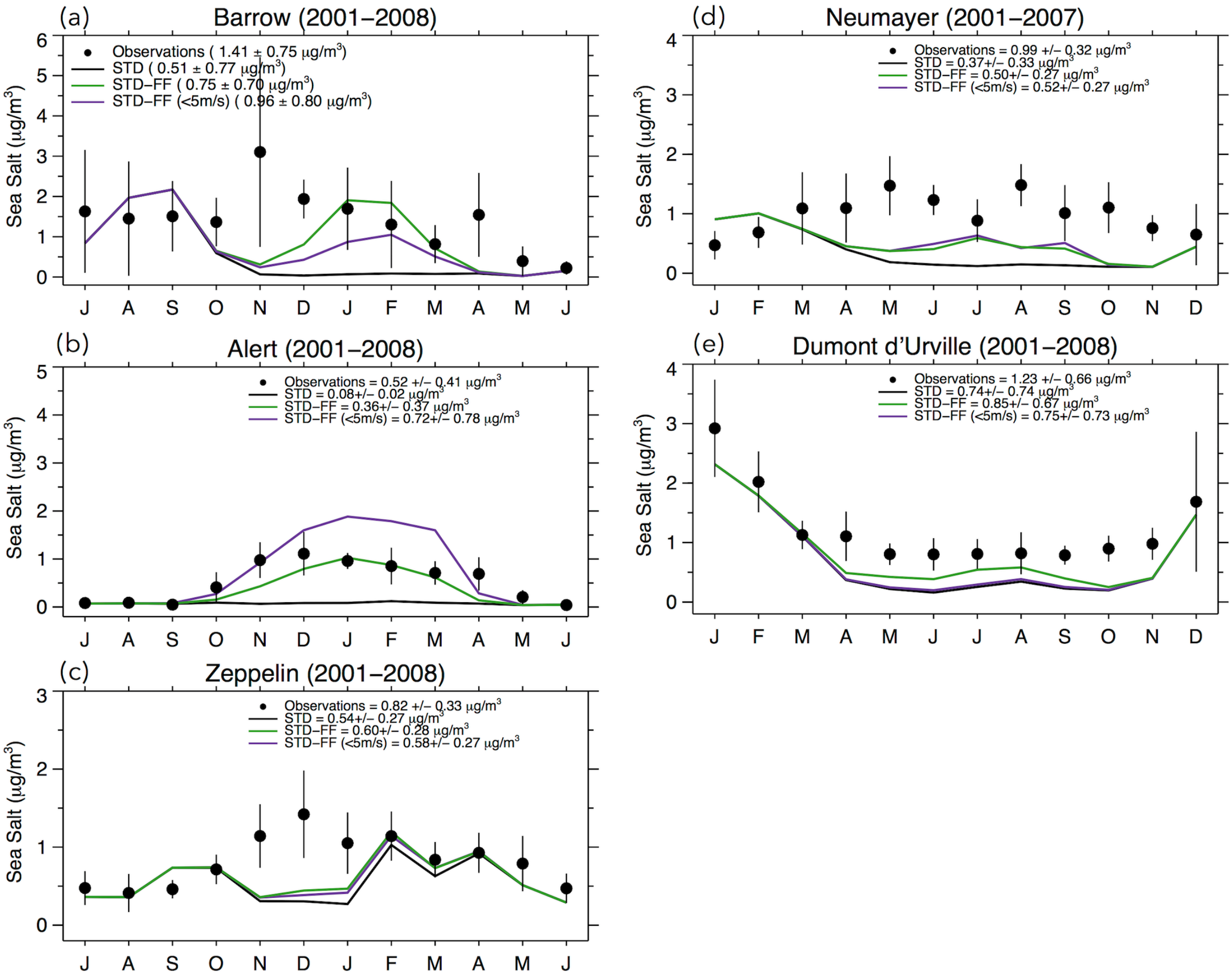

Figure S3: Monthly mean surface SSA mass concentrations at (a) Barrow, (b) Alert, (c) Zeppelin, (d) Neumayer and (e) Dumont d'Urville. The observed mean concentrations are indicated with filled black circles, while the black line is for the GEOS-Chem model with open ocean emissions (STD) and the green line is for the frost flower simulation. We also show a sensitivity simulation in which we impose a 5 m/s wind threshold beyond which frost flower emissions are suppressed: STD-FF (<5m/s) (purple line). The black vertical lines and for each individual panel, the legend lists mean concentrations and standard deviations.

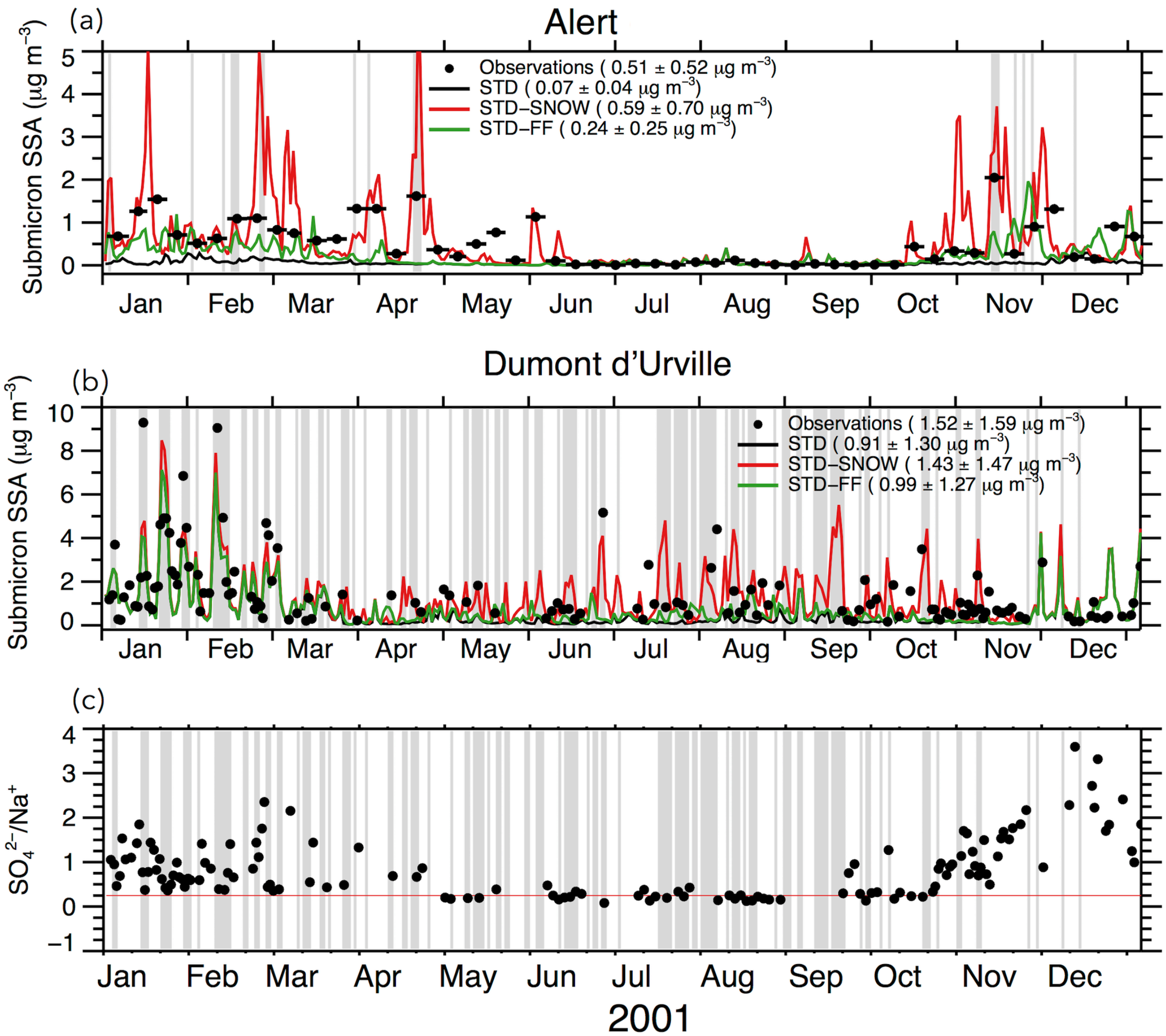

Figure S4: Weekly/daily variations in SSA mass concentrations at Alert (a) and Dumont d'Urville (b) for 2001. Observations are shown with black circles, while the GEOS-Chem simulations are indicated with lines (STD: black, STD-SNOW: red, and STD-FF: green). Also shown in the daily variations of sulphate to sodium ratio as observed at Dumont d'Urville (c) for 2001. The red line indicates the SO_4^{2-}/Na^+ of 0.25 in seawater. Shaded grey areas in (a-c) indicate time periods when local u_{10m} exceeds the blowing snow wind threshold.

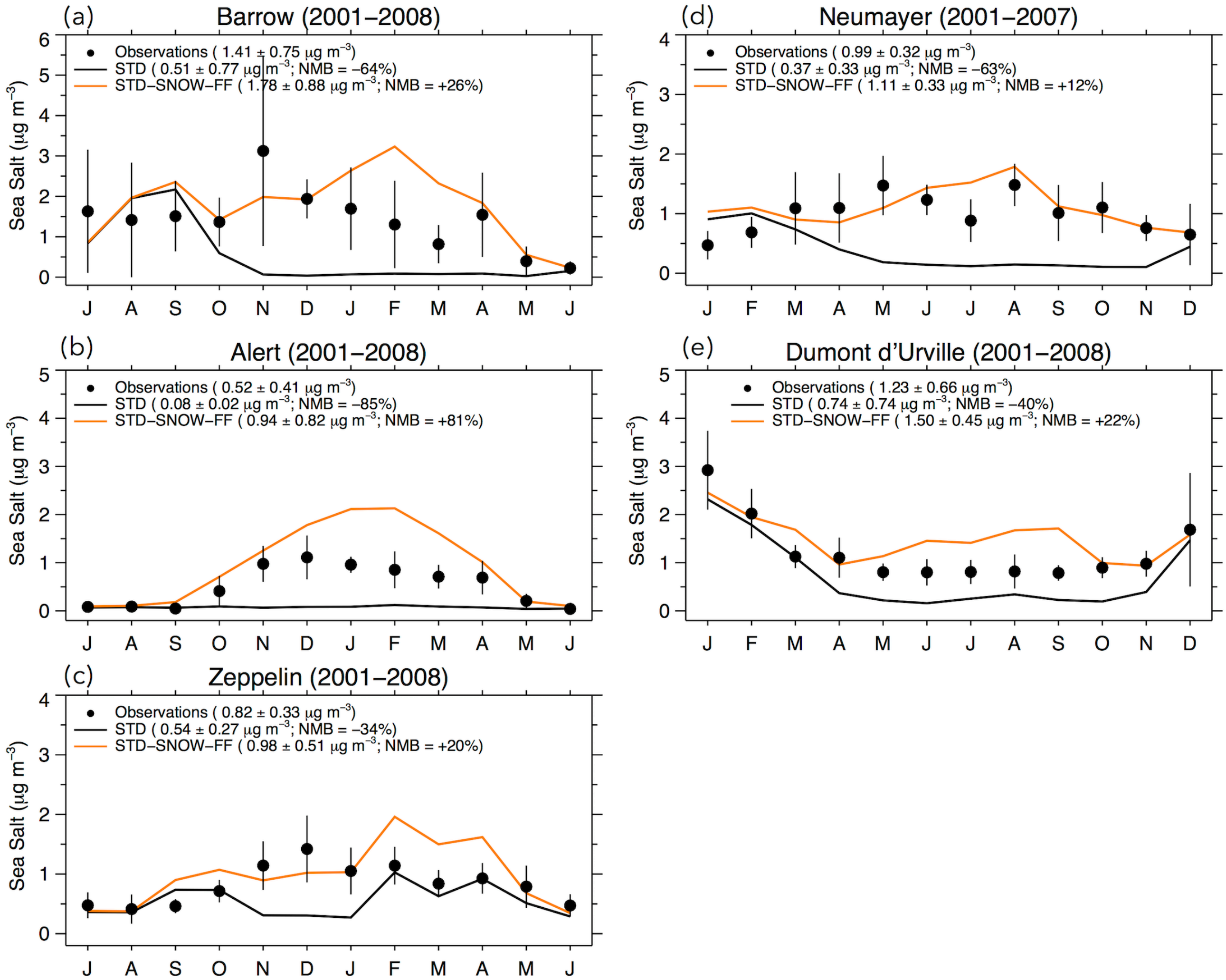

Figure S5: Monthly mean surface SSA mass concentrations at (a) Barrow, (b) Alert, (c) Zeppelin, (d) Neumayer and (e) Dumont d'Urville. The observed mean concentrations are indicated with filled black circles, while the lines are for the GEOS-Chem model. The black line is for open ocean simulation (STD), while the orange line is when all tree SSA sources are included (open ocean, blowing snow, and frost flowers). The black vertical lines and for each individual panel, the legend lists mean concentrations and standard deviations.